JOM, Vol. 64, No. 2, 2012
DOI: 10.1007/s11837-012-0244-1

The Effect of Alloying Elements on the Microstructure of Al-5Fe Alloys

BO LIU,[1,2,3] XIAO-GUANG YUAN,[2,4] HONG-JUN HUANG,[2] and ZHIQIANG GUO[2]

1.—School of Naval Architecture and Civil Engineering, Zhejiang Ocean University, Zhoushan 316000, China. 2.—School of Materials Science and Engineering, Shenyang University of Technology, Shenyang 110870, China. 3.—e-mail: Liubo@zjou.edu.cn. 4.—e-mail: Yuanxg630121@gmail.com

The effects of adding Cr, Mn, and Zr on the microstructure of Al-5Fe alloys has been studied by metallographic analysis, scanning electron microscopy, x-ray diffraction analysis, and differential thermal analysis. It has been found that the effects of the different elements on the microstructure of ferro-aluminum intermetallics in Al-5Fe alloys are not alike. Addition of Cr in Al-5Fe alloys dissolves only into AlFe intermetallics, resulting in the morphology of the AlFe phases being changed with increasing Cr content. Cr is a favorable nucleating agent for encouraging metastable Al_xFe (x = 4.6 to 5.0) phase formation. Adding Mn in Al-5Fe alloys may stabilize the metastable Al_6Fe phase, helping the primary phase field of Al_7Cr diminish or even disappear and forcing Cr to dissolve into AlFe phases. Adding Zr does not refine the primary AlFe intermetallics. Al_3Zr particles in Al-5Fe alloys will occupy the growing spaces of ferro-aluminum phases and indirectly hinder the growth of Fe-bearing phases.

INTRODUCTION

The increasing demand for stronger, lightweight materials at elevated temperatures has led to the development of new aluminum alloys. Some of the most popular are precipitation strengthened alloys, which are easy to process. The drawback of many of these alloys is that they are restricted to relatively low temperature use (<150°C), because of the dissolution and/or rapid coarsening of the precipitates.[1,2] Al-TM (TM = transition metals, such as Fe, Cr, Mn, and Zr) alloys represent an exception because they can form stable intermetallics which have low diffusivity in the Al matrix. The cuboidal $Al_{13}TM_4$ precipitates that form remain stable at elevated temperatures.[3]

In Al-Fe alloys, the compound $Al_{13}Fe_4$ (denoted by Al_3Fe or θ-phase) forms directly from the alloy melt at about 1160°C,[1,4] and the mechanical properties of the alloys are strongly dependent upon the size, morphology, and distribution of this compound. Coarse crystals of $Al_{13}Fe_4$ tend to crack and produce notches that reduce the formability and fatigue resistance, whereas finely dispersed $Al_{13}Fe_4$ can greatly improve alloy properties. The published methods to alter the size and morphology of $Al_{13}Fe_4$ include rapid solidification,[5–9] unidirectional solidification,[10,11] and addition of alloying elements or master alloys.[11–18]

The fact that addition of alloying elements can change the size and morphology of iron-containing intermetallics has been demonstrated by many researchers. Zhou and Li et al.[14–16] considered that the morphology of primary Al_3Fe phase in Al-5Fe alloy is improved appreciably due to alloying element additions. Al_3Fe without Cr mainly appears as bulky needle-like, needle–plate-like, or small flower-like precipitates, and is changed into small needle-like and needle–dot-like forms after adding 0.2% to 1.0% Cr (all concentrations in mass percent unless otherwise stated). Addition of 2.5% Mn and 0.I% Mg changes the primary Al_3Fe phase from thick needle-like to fine needle-like, particle-like, and flower-like forms; however, addition of 2.5% Mn and 1.5% Mg forms particle-like and fringe-like precipitates. Cr mainly distributes in the primary Al_3Fe phases, and Mg mainly in the matrix. Sahoo et al.[13] found that an Al-8.3Fe-0.8V-0.9Si alloy melt treated with 1.5% of Mg or 1.0% of Ni-20%Mg master alloy could alter the star-shaped morphology of the $Al_{13}Fe_4$ precipitates to rectangular, hexagonal, or other compact forms. According to studies by

(Published online February 11, 2012)

Huang et al.,[17] when 2.6% Mn was added to spray-forming Al-20Si-5Fe alloy, needle-shaped Al_4FeSi_2 and Al_5FeSi intermetallics would be altered to form particulate $Al_{15}(Fe,Mn)_3Si_2$ in the deposited perform. In Al-20Si-2.5Fe-2.5Mn alloy, however, $Al_4(Fe,Mn)Si_2$, $Al_5(Fe,Mn)Si$, and $Al_{15}(Fe,Mn)_3Si_2$ phases coexisted in the alloy by oversprayed powders, whereas only particulate $Al_{15}(Fe,Mn)_3Si_2$ phase could be observed in the deposited perform, and mechanical properties were improved.

However, there is little literature on the structure and morphology of iron-containing phases formed in the multicomponent Al-Fe system during conventionally casting. In the present work, we aim to investigate the interaction of elements, such as Cr, Mn, and Zr, added to hypereutectic Al-5Fe alloy, to understand the effect of the alloying elements on the microstructure of conventionally cast Al-5Fe alloys and clarify the morphology and formation mechanism of the Fe-rich intermetallics.

EXPERIMENTAL PROCEDURES

The alloys were prepared in a well-type resistance furnace whose power was 30 kW and temperature limit was 1000°C. An appropriate amount of pure Al (99.5%) and master alloys (Al-20%Fe, Al-10%Cr, and/or Al-10%Mn) was heated to 830°C to 850°C using a graphite crucible in the electric furnace. Al-5%Zr master alloy and the remaining raw materials were added to the crucible after the metals were melted; the melt was covered with mixed salt composed of 55 KCl and 45 NaCl, then heated to 830°C to 850°C and held for 30 min. When the alloy was quite molten, the crucible was removed from the furnace, stirred using a SiC rod, degassed by dry C_2Cl_6 tablet, and held for 10–15 min in the furnace. After the gas had fully escaped, the dross was cleaned off and the metal stirred. Two graphite molds of different sizes were used for casting: ϕ 85 $\times$ 32 mm and ϕ110 $\times$ 72 mm.

HF solution (0.5%) was used for etching to reveal the microstructure, following the standard metallographic preparation process. Scanning electron microscopy (SEM) examination was done with a Hitachi S-3400 N SEM equipped with Oxford energy-dispersive x-ray spectroscopy (EDS). The phases were identified by using a Bruker D8 Discover x-ray diffractometer (XRD) using Cu $K_{\alpha 1}$ radiation. Differential thermal analysis (DTA) was carried out using a Dupont-1090 thermal analyzer over a temperature range from 300°C to 900°C, under a constant heating rate of 10°C/min.

RESULTS AND DISCUSSION

The Microstructure of Al-5Fe Alloy

An as-cast microstructure of binary Al-5Fe alloy poured into the smaller graphite mold is shown in Fig. 1. It can be seen that the microstructure of as-cast Al-5Fe alloy is mainly composed of α-Al matrix and iron-rich phase, which also agrees with the XRD result of the as-cast binary alloy.[19] Figure 1 shows the quite different morphology of the iron-rich phases in the sample because of the various solidification conditions at different sample locations. In some areas with lower solidifying rate or Fe-rich, bulk platelet intermetallic form (Fig. 1a–c), and in other large areas with higher solidifying rate, only thinner and shorter iron-rich phase exists (Fig. 1a, b). Moreover, also revealed are not quite regular ten-armed star-shaped or polygonal star-shaped precipitates in the Al matrix (Fig. 1b, c), in agreement with previous studies.[13,20] This implies that twinning is a major growth route of Al_3Fe intermetallic phase in Al-Fe alloys. Furthermore, Fig. 1 also reflects that the size and distribution of the iron-rich phase at different sample locations are not uniform. They have sharp edges and corners, and their growth has certain directivity. In fact, the iron-rich phases formed in hypereutectic Al-Fe alloys are related not only to the cooling rate but also to the Fe content.[10] More accurately, they should be related to the local solidifying rate.[11] Al_3Fe clusters could have originated from ten-pointed stars whose arms have grown to such an extent that they are separated from the nucleus of the star.[20] The first stages of this process can be seen in Fig. 1a, c, where some of the arms have already become

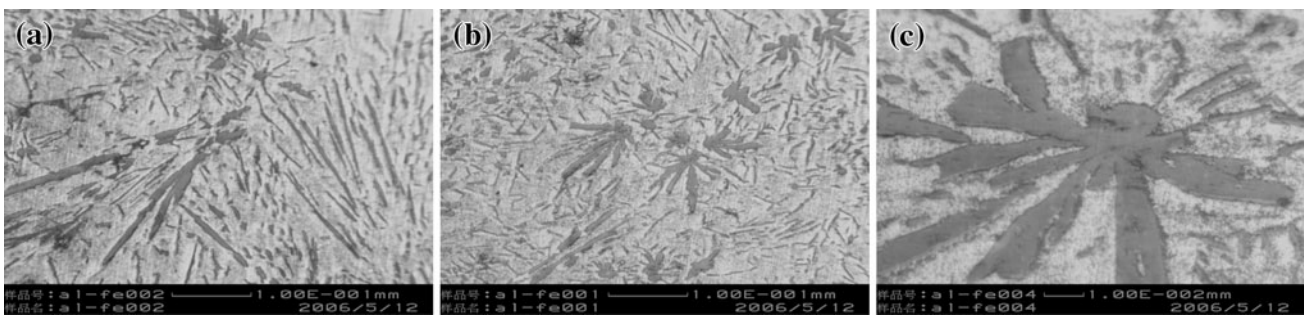

Fig. 1. As-cast microstructures of binary Al-5Fe alloy.

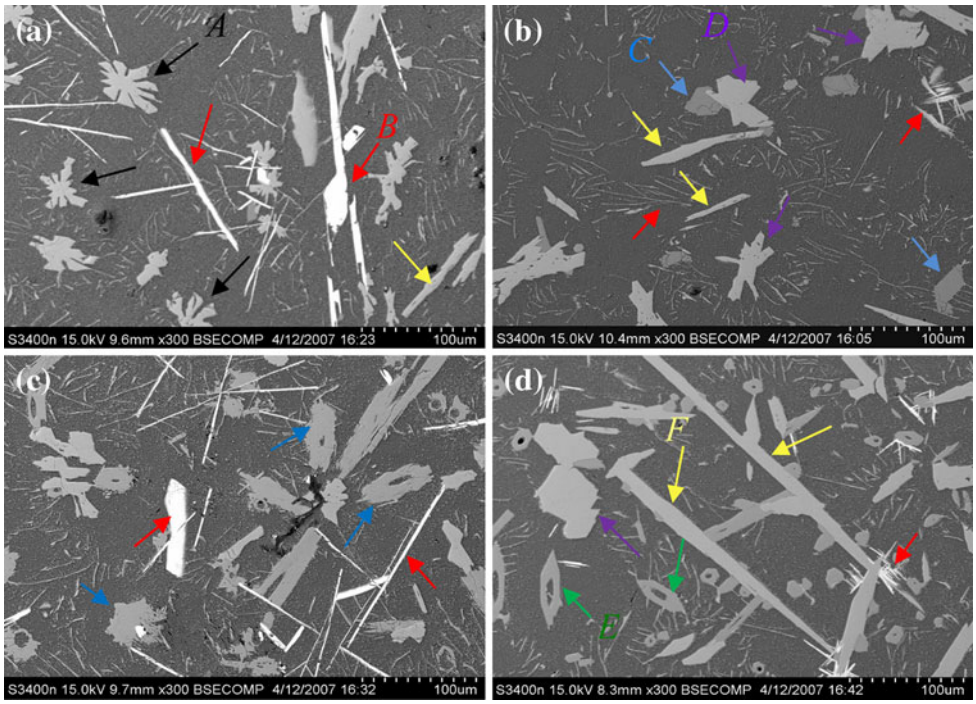

Fig. 2. As-cast microstructures of Al-5Fe-1.7Zr-*X*Cr alloy: (a, b) 1% Cr, (c) 2% Cr, and (d) 3% Cr. Marks of the same color indicate similar phase (Color figure online).

separated from the nucleus. In addition, the coarse iron-rich phase has seriously segregated the matrix and will cause the mechanical properties of the final alloy to decrease.

The Effect of Cr, Mn, and Zr on the Microstructure

A series of increasing Cr contents (1%, 2%; and 3%) were applied to explore the influence of Cr on the morphology of the formed primary iron-rich phase and microstructure in Al-5Fe-1.7Zr-*X*Cr alloys. Figure 2 presents SEM images of the as-cast alloys poured in the larger graphite mold, with different Cr contents. As shown in Fig. 2a, irregular star-like iron-rich intermetallic θ-$Al_{13}Fe_4$ exists in the microstructure of the specimen and nearly dominates the microstructure. After addition of 1% Cr, polygonal θ-AlFe(Cr) phase and polylateral AlFe(Cr) intermetallic phases appear in the microstructure (Fig. 2b). The polylateral intermetallic consists of 83.27 at.% Al, 8.61 at.% Fe, and 8.12 at.% Cr, and the stoichiometry is close to $Al_{4.98}$(FeCr) (C in Table I). This is a metastable phase of Al_xFe (x = 4.6 to 5.0) type, in which the Fe atoms on the Al_xFe lattice can be replaced by other atoms.[21] As shown in Fig. 2c, the stellate θ-phase nearly disappears and the θ-AlFe(Cr) phase appears in the microstructure with increasing Cr content up to 2%. While the amount of θ-AlFe(Cr) intermetallics increases, the morphology of intermetallics tends to form a ring. As shown in Fig. 2d, the θ-AlFe(Cr) phase still exists, but the phase shape changes to coarse sheet-like in the microstructure with increasing Cr content up to 3%. The morphology of the AlFe(Cr) intermetallics becomes ring form, and its constituents change, made up of 82.27 at.% Al, 11.21 at.% Fe, and 6.52 at.% Cr, with stoichiometry close to $Al_{4.64}$(FeCr) (E in Table I). As the Cr content increases, the θ-AlFe(Cr) phase changes from needle-like without Cr to polyangle-like with low Cr and then to sheet-like with high Cr, while the transition of AlFe(Cr) phase is from polygon-like to ring-like. This indicates that addition of small amounts of Cr (~1%) may encourage twinning of the $Al_{13}Fe_4$ phase, resulting in the formation of stellate $Al_{13}Fe_4$ phase, and then Cr may dissolve in the AlFe(Cr) phases, leading to varying growth of the phase.

Figure 3 shows an as-cast microstructure of Al-5Fe-2Cr-1Mn-1Zr alloy. The $Al_{13}Fe_4$ phase has reduced in thickness, shortened, reduced in amount, and varied in growth direction compared with the as-cast microstructure of Al-5Fe alloy (Fig. 1) after adding Mn, Zr, etc. elements. There are many lump-like and ring-like phases in the microstructure of the alloy. The EDS result indicates that these compounds are AlFe(Cr) intermetallics with or without Mn (Table II). The quantity of these phases was greatly increased, accounting for almost 50% of the second phase, and the distribution was more uniform (Fig. 3). However, the size of the AlFe(Cr) phases in the microstructure of the alloy is essentially of the same magnitude as in the microstructure of the Al-5Fe-3Cr-1.7Zr alloy (Fig. 2). The

Table I. Results of EDS analysis of phases shown in Fig. 2

Mark	Content (at.%)				Stoichiometry	Morphology in 2D View
	Al	Fe	Cr	Zr		
A	79.42	20.58	–	–	$Al_{13}Fe_4$	Polygonal star-like
B	75.01	–	–	24.99	Al_3Zr	Bright white needle shape
C	83.27	8.61	8.12	–	$Al_{4.98}(FeCr)$	Multilateral shape
D	77.91	20.03	2.06	–	$Al_{13}(Fe,Cr)_4$	Polygonal shape
E	82.27	11.21	6.52	–	$Al_{4.64}(FeCr)$	Ring-like
F	75.73	20.48	3.79	–	$Al_{13}(Fe,Cr)_4$	Acicular

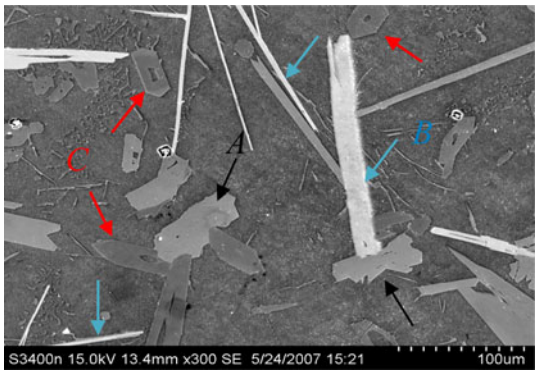

Fig. 3. As-cast microstructure of Al-5Fe-2Cr-1Mn-1Zr alloy.

presence of the α-Al, $Al_{13}Fe_4$, and Al_3Zr phases was clearly seen in the x-ray spectrograms of the Al-5Fe-3Cr-1Mn-1Zr alloy (Fig. 4). X-ray peaks of $Al_{13}Fe_4$ phase are slightly shifted due to Cr dissolved in $Al_{13}Fe_4$. There are no binary AlCr compounds in the spectra. Additional weak x-ray peaks were observed at 2θ values of about 18.09°, 20.11°, 20.71°, 22.48°, 23.75°, 27.20°, 34.35°, 35.58°, 39.34°, 39.93°, 41.19°, 42.10°, 43.34°, 62.20°, and 74.64° for the alloy. Whether these peaks can be assigned to the distorted $Al_xFe(Cr)$ phase remains to be determined. The relatively weak and broad x-ray peaks and considerable amount of diffuse background intensity demonstrate that the structure of this alloy is disordered. Thus, the effect of alloying element additions on the microstructure of Al-5Fe alloys is large.

When Zr was added to the Al alloys it formed Al_3Zr particles, and minor Al_3Zr can refine Al grains. If there is a higher quantity of Zr, the Al_3Zr phase in the Al-5Fe alloys is seen as shiny white fine needle-like and large lamellar-like structures (Figs. 2, 3). These fine needle-like Al_3Zr phases grow around Fe-containing intermetallics or both ends of lamellar Fe-rich phases and would block off the intermetallics from further growth.

The Role of Cr, Mn, and Zr in Structural Formation

Cr added in Al-5Fe alloy melt will only dissolve in Al-Fe intermetallics because the solubility of Cr in the Al–Fe intermetallics is much higher than in the Al matrix.[1,2,22] The DTA of Al-5Fe-3Cr-1Mn-1Zr alloy shows only one endothermic peak between 645.2°C and 680.5°C (Fig. 5), for which the starting temperature of the eutectic reaction is slightly higher and the temperature range is narrower compared with that in DTA of Al-5Fe alloy.[19] This also demonstrates that the added Cr prefers to dissolve in the AlFe binary phases rather than to form AlCr binary compound.

Previous work[10,20,23] considered that metastable phases Al_xFe, Al_6Fe, Al_mFe, and Al_9Fe_2 and the equilibrium phase $Al_{13}Fe_4$ could form in binary and multicomponent Al-Fe alloys, and that one of these phases appeared depending upon the alloy composition and the cooling rate during solidification. The equilibrium phase $Al_{13}Fe_4$ was observed only at a low cooling rate, while Al_xFe, Al_6Fe, Al_mFe, and Al_9Fe_2 appeared in sequence on increasing the cooling rate during solidification. The cooling rate range of formation of the Al-Al_xFe eutectic in Al-Fe alloys is 0.4°C/s to 5°C/s between the Al-Al_3Fe and Al-Al_6Fe eutectic. The cooling rate in the present work is around 1.5°C/s, enabling the formation of the Al-Al_xFe eutectic. The investigators of Refs. [15] and [19] observed the formation of the phases of Al-5Fe-1.6Cr-1Mg and Al-5Fe-2Cr alloy, which were poured in a chill mold (60 mm long, 12 mm diameter) with cooling rate of about 10^2°C/s.[19] In general, only metastable Al_6Fe or Al_mFe (m = 4 to 4.4) phases can form at such a high cooling rate.[11,21] However, it has been found that the Al_xFe phase also exists in these alloys, in addition to Al_6Fe phase (Table III). Thus, it can be seen that Cr is a favorable nucleant for Al_xFe formation because the formation of the Al_xFe phase is sensitive to the nucleation conditions present preceding growth.[11]

Slight addition of Cr (~1%) has the effect of increasing the cooling rate, and can facilitate the primary θ-AlFe compound to form stellate structure and to feed metastable Al_xFe intermetallic. This is a reason why Cr can cause a degree of supercooling of the growth dynamics to produce or increase compositional undercooling. Cr dissolving in θ-AlFe(Cr) phase would occupy the position of Fe atoms prior to growth, forcing the Fe atoms to shift position to suboptimal growth, so the aspect ratio of the morphology of θ-AlFe(Cr) phase decreases, tending to

Table II. Results of EDS analysis of phases shown in Fig. 3

Mark	Content (at.%)					Stoichiometry	Morphology in 2D View
	Al	Fe	Mn	Cr	Zr		
A	83.15	6.99	3.10	6.77	–	$(Al,Mn)_6(Fe,Cr,Mn)$	Blocky
B	74.71	–	–	–	25.29	Al_3Zr	Bright white needle shape
C	82.17	11.30	–	6.53	–	$Al_{4.61}(FeCr)$	Ring-like

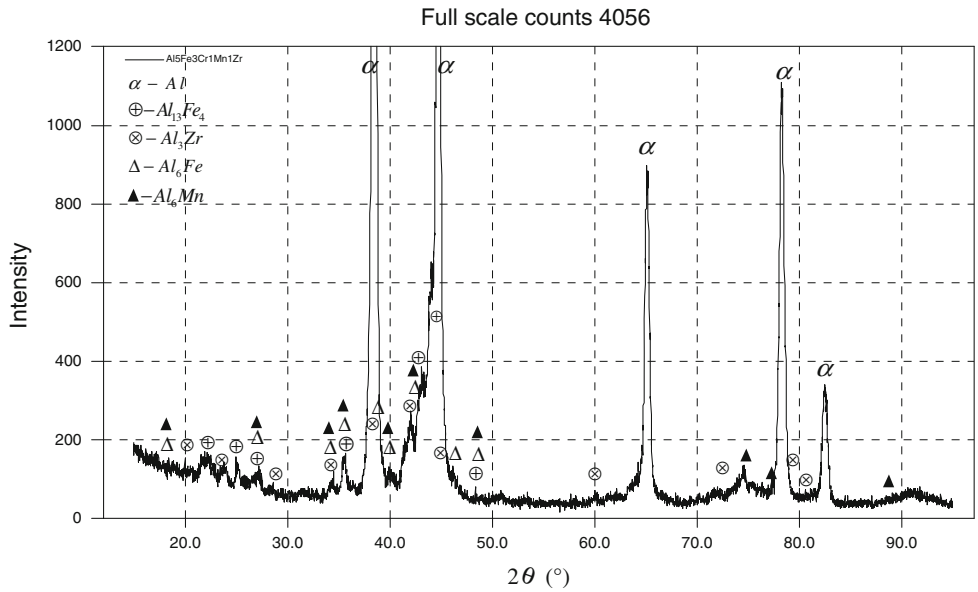

Fig. 4. X-ray diffraction pattern of Al-5Fe-3Cr-1Mn-1Zr alloy.

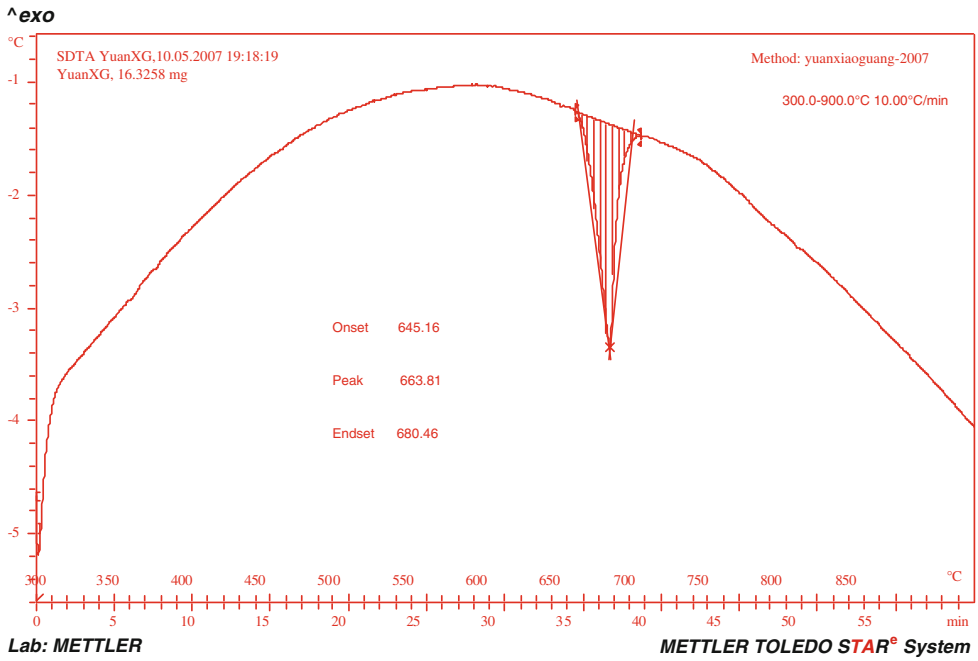

Fig. 5. DTA curve of Al-5Fe-3Cr-1Mn-1Zr alloy.

Table III. Results of EDS analysis of phases from Al-5Fe-1.6Cr-1Mg[15] and Al-5Fe-2Cr[19] alloys

Alloy	Content (at.%)			Stoichiometry	Morphology in 2D View
	Al	Fe	Cr		
Al-5Fe-1.6Cr-1Mg	83.43	11.76	4.81	$Al_{5.04}(FeCr)$	Polylateral-like
Al-5Fe-2Cr	85.85	9.52	4.63	$Al_{6.06}(FeCr)$	Plate-like
Al-5Fe-2Cr	84.06	10.68	5.26	$Al_{5.27}(FeCr)$	Polylateral-like

form a polygon. As the Cr content increases, the phase could integrate more Cr, causing the liquid phase of the solidification front to become enriched with Fe, resulting finally in θ-AlFe(Cr) phase regrowth along the preferred direction and the size of the θ-AlFe(Cr) phase to increase further. While the metastable Al_xFe phase is a defect structure,[23] this implies that a greater amount of Cr can be integrated than the stable θ-AlFe phase. More Cr dissolved in AlFe(Cr) phase can occupy the position of Fe atoms and the defects, so as to decrease the volume energy of the phase and form multilateral-shape or ring-like structure.

In contrast to other transition elements, the solubility of Mn in Al is high, being up to 1.8% at 658°C.[1,2] Added 1% Mn in this alloy would dissolve mostly in the Al matrix before solidification. However, introduction of Mn may stabilize the metastable Al_6Fe phase, and promote Al_6Fe and Al_6Mn phase coprecipitation, forming orthorhombic $Al_6(FeMn)$ continuous solid solution and resulting in the decrease or even disappearance of the primary phase field of Al_7Cr.[2,18] Thus, it is evident that adding a small amount of Mn in this alloy would stabilize the metastable Al_6Fe phase and make the Al_7Cr phase disappear. This will drive the formation of $Al_6(FeMn)$ phase and lead to Cr dissolving more in AlFe phase. XRD of Al-5Fe-3Cr-1Mn-1Zr alloy confirms this result (Fig. 4).

The solubility of Zr in Al is very low (0.083 at.% at 660.8°C[24]) and is improved by adding Mn. A small amount of Zr does not form compounds with Fe, Mn, or Cr in the Al-5Fe alloys, and the solubility of Zr in binary iron, manganese, and chromium aluminide is negligible.[8,24–29] As a result, a small amount of Zr can only form Al_3Zr with Al in the Al-5Fe alloys. Each of the Al_3Fe and Al_3Zr phases singly precipitates from the liquid at high temperature and forms a α-Al + Al_3Fe + Al_3Zr eutectic at about 650°C during solidification.[1,26] Although the melting point of Al_3Zr is higher than that of Al_3Fe, the primary Al_3Zr particles precipitated from the melt have the stable, tetragonal $D0_{23}$ structure or the metastable, cubic $L1_2$ structure, and the structure of these particles is different from the Al_3Fe phases with monoclinic structure. It is difficult to form a coherent heterogeneous interface of very low interfacial energy. Therefore, Al_3Zr does not become the core of Al_3Fe heterogeneous nucleating. As a consequence, added Zr cannot refine the primary Al_3Fe phases. However, the precipitation of abundant fine needle-like Al_3Zr phase would occupy the growing spaces of AlFe phases, and change the component of solute ahead of the AlFe phase interface to hinder growth of Fe-bearing phases indirectly.

CONCLUSIONS

Cr is a favorable nucleant for encouraging metastable Al_xFe (x = 4.6 to 5.0) phase formation. The Al_xFe phase may incorporate more Cr than the stable θ-AlFe phase. The morphology of the metastable AlFe(Cr) phase transforms from polygon-like to ring-like with increasing Cr content. Addition of a small amount of Cr (~1%) may cause a degree of supercooling to produce or increase compositional undercooling, and can facilitate the primary θ-AlFe compound to form stellate structure. In Al-5Fe alloys, Cr prefers to dissolve in the AlFe binary phases rather than to form AlCr binary compound. As the Cr content increases, stable θ-AlFe(Cr) phase changes from needle-like structure without Cr to polyangle-like structure with low Cr, then to sheet-like structure with high Cr. The size of the phase is first decreased and then increased with increasing Cr content.

Addition of a certain amount of Mn in Al-5Fe alloys may stabilize the metastable Al_6Fe phase and cause formation of $Al_6(FeMn)$ continuous solid solution. Introduction of Mn in the alloys can make the primary phase field of Al_7Cr diminish, or even disappear, and force Cr to dissolve in the AlFe phase. This would change the morphology and growth of Fe-containing phases.

The Al_3Zr particles exist independently in the Al-5Fe alloys. These particles do not become the core of the primary AlFe intermetallics and cannot refine the primary phases. However, precipitation of abundant fine needle-like Al_3Zr phase in the alloys would occupy the growing spaces of AlFe phases, change the component of solute ahead of the AlFe phase interface, and hinder the growth of Fe-bearing phases indirectly.

ACKNOWLEDGEMENTS

The authors are grateful to Liaoning Province Science and Technology Plan, China, for financial support under Contract No. 2010221007 and support by the Program for Liaoning Excellent Talents in University, China, 2008RC36.

REFERENCES

1. L.F. Mondolfo, *Aluminium Alloys: Structures and Properties* (London: Buttorworths, 1976).
2. V.S. Zolotorevsky, N.A. Belov, and M.V. Glazoff, *Casting Aluminum Alloys* (Oxford: Elsevier, 2007).
3. B. Grushkoa and T. Velikanova, *Calphad* 31, 217 (2007).
4. U.R. Kattner and B.P. Burton, *Al-Fe (Aluminum-Iron). ASM Metals Handbook Volume 3—Alloy Phase Diagrams* (Materials Park, OH: ASM International, 1992), pp. 294–295.
5. X.F. Bian, X.M. Pan, C. Zhao, and S.J. Yuan, *Mater. Sci. Technol.* 17, 917 (2001).
6. A. Griger and V. Stefániay, *J. Mater. Sci.* 31, 6645 (1996).
7. J.D. Cotton and M.J. Kaufman, *Metall. Trans. A* 22A, 927 (1991).
8. Y.H. Zhang, Y.C. Liu, Y.J. Han, C. Wei, and Z.M. Gao, *J. Alloys Compd.,* 473, 442 (2009).
9. E.M. Sokolovskaya, L.M. Badalova, E.I. Poddýakova, E.F. Kazakova, and S.I. Borovikova, *Met. Sci. Heat Treat.* 30, 606 (1988).
10. I.R. Hughes and H. Jones, *J. Mater. Sci.* 11, 1781 (1976).
11. C.M. Allen, K.A.Q. O'Reilly, B. Cantor, and P.V. Evans, *Prog. Mater. Sci.* 43, 89 (1998).
12. H.Y. Hsieh, B.H. Toby, T. Egami, Y. He, S.J. Poon, and G.J. Shiflet, *J. Mater. Res.* 5, 2807 (1990).
13. K.L. Sahoo, S.K. Das, and B.S. Murty, *Mater. Sci. Eng. A* 355, 193 (2003).
14. Z.P. Zhou, R.D. Li, J.C. Ma, and X.G. Yuan, *J. Mater. Eng.* Z1, 20 (2006).
15. R.D. Li, S.Y. Zhao, and Z.P. Zhou, *J. Shenyang Univ. Technol.* 30, 284 (2008).
16. Z.P. Zhou and R.D. Li, *Acta Metallurgica Sinica* 39, 608 (2003).
17. H.J. Huang, Y.H. Cai, H. Cui, J.F. Huang, J.P. He, and J.S. Zhang, *Mater. Sci. Eng. A* 502, 118 (2009).
18. Z. Homonnay, A. Vièrtes, Á. Cziráki, Á. Oszkó, G.Y. Menczel, and L. Murgás, *J. Radioanal. Nucl. Chem.* 139, 127 (1990).
19. Z.P. Zhou (Ph.D dissertation, Shenyang University of Technology, Shenyang, 2008) (in Chinese).
20. E. Louis, R. Mora, and J. Pastor, *Met. Sci.* 14, 591 (1980).
21. R.M.K. Young and T.W. Clyne, *Scripta Metall.* 15, 1211 (1981).
22. V. Raghavan, *J. Phase Equilb.* 24, 257 (2003).
23. P. Skjerpe, *Metall. Trans. A* 18A, 189 (1987).
24. J. Murray, A. Peruzzi, and J.P. Abriata, *J. Phase Equilb.* 13, 278 (1992).
25. V. Raghavan, *J. Phase Equilb. Diffus.* 30, 620 (2009).
26. V. Raghavan, *J. Phase Equilb. Diffus.* 27, 284 (2006).
27. V. Raghavan, *J. Phase Equilb. Diffus.* 31, 459 (2010).
28. T. Ohashi and R. Ichikawa, *Bull. Nagoya Inst. Technol.* 22, 383 (1970).
29. M. Vlach, I. Stulíková, B. Smola, and N. Žaludová, *Mater. Charact.* 61, 1400 (2010).